ORIGINAL RESEARCH

Effect of Puerarin on Osteogenic Differentiation in vitro and on New Bone Formation in vivo

Yanran Yang[1], Daiyun Chen[2], Yilin Li[1], Jinghua Zou[1], Ruiqi Han[1], Hongkun Li[1], Jun Zhang[1]

[1]Shandong University & Shandong Key Laboratory of Oral Tissue Regeneration & Shandong Engineering Laboratory for Dental Materials and Oral Tissue Regeneration, Department of Orthodontics, School and Hospital of Stomatology, Cheeloo College of Medicine, Shandong University, Jinan, People's Republic of China; [2]Department of Orthodontics, School of Stomatology, Shandong First Medical University, Jinan, People's Republic of China

Correspondence: Jun Zhang, Shandong University & Shandong Key Laboratory of Oral Tissue Regeneration & Shandong Engineering Laboratory for Dental Materials and Oral Tissue Regeneration, Department of Orthodontics, School and Hospital of Stomatology, Cheeloo College of Medicine, Shandong University, Jinan, People's Republic of China, Tel +86 13953109816, Fax +86 53188382923, Email zhangj@sdu.edu.cn

Purpose: Puerarin ($C_{21}H_{20}O_{10}$) is a phytoestrogen that possesses various pharmacological effect, and several researches have revealed the relationship between puerarin and bone metabolism. This study was aimed to evaluate the potential influence of puerarin on the proliferation and osteogenic differentiation of rat bone marrow-derived mesenchymal stem cells (BMSCs) as well as on new bone formation following rapid maxillary expansion (RME) model in rats.

Methods: Rat BMSCs were adopted, and the cell proliferation was detected by cell-counting kit-8 (CCK-8) assay in vitro experiments. Alkaline phosphatase (ALP) activity and alizarin red staining were analyzed quantitatively to show extracellular matrix mineralization. The mRNA and protein expression levels were used to detect osteogenic differentiation of BMSCs. In vivo bone regeneration was analyzed in a rat RME model. Eighteen 6-week-old male Wistar rats were divided into 3 groups: group 1 without any treatment, group 2 received RME and saline solution (15mg/kg), group 3 received RME and puerarin solution (15mg/kg). After 2 weeks, micro-computed tomography (Micro-CT), hematoxylin and eosin (HE) staining, and Masson staining were used to detect the new bone formation and morphological changes. Besides, ALP and bone morphogenetic protein 2 (BMP2) expression levels in mid-palatal suture were evaluated by immunohistochemical staining.

Results: The results showed that puerarin upregulates cell proliferation dose-dependently. ALP activity and mineralized matrix generation were clearly enhanced at certain specific concentrations (10^{-5} and 10^{-6} mol/L); the expression levels of the osteoblast-related genes and proteins were increased. The measurement of micro-CT imaging revealed that puerarin significantly promoted new bone formation. Concomitantly, the histological examinations showed that puerarin solution enhanced osteogenesis in mid-palatal suture.

Conclusion: Those works indicated that puerarin regulates osteogenesis in vitro and exerts a beneficial impact on bone regeneration in vivo, revealing that puerarin treatment may become one of the potential keys for improving the stability and preventing relapse of RME.

Keywords: bone marrow-derived mesenchymal stem cells, bone regeneration, micro-CT, rapid maxillary expansion

Introduction

As scholars have been studying tissue engineering more and more, oral bone regeneration which is of fundamental importance in the dentistry field has become a hot research topic.[1] Mesenchymal stem cells (MSCs) are undifferentiated cells known for their self-renewal and differentiation properties, and they can secrete immunomodulatory factors, leading to the creation of a regenerative microenvironment, and trans-differentiate into cells of the different germ layers: mesoderm lineage cells, as well as ectoderm and endoderm lineage cells.[2] The capacity of MSCs is useful for osteogenic differentiation and tissue regeneration.[3] Some clinical studies have demonstrated that MSCs from different sources may have the ability to repair, replace, and regenerate cells, tissues, and bones.[4] MSCs can be extracted from different tissues such as bone marrow, skeletal muscle, cartilage, dental organ, adipose tissue, synovium, and cardiac tissue.[5] BMSCs were the first to be discovered.[6] Bone is formed via endochondral and intramembranous ossification.[7] MSCs play a vital

role in bone formation. On the one hand, MSC-driven condensation occurs firstly, and then, MSCs differentiate into chondrocytes during the process of formation of growth plates, which are replaced by new bone in longitudinal-endochondral bone growth.[8] On the other hand, MSCs can also directly differentiate into osteoblasts in bone formation such as skull, facial bones, and pelvis, generated by intramembranous ossification without a cartilaginous template.[9,10]

Transverse maxillary constriction often manifests a typical vertical skeletal pattern, with long anterior lower facial height, high palatal vault, low tongue posture, incompetent lip muscles, and mouth-breathing.[11] Previous studies indicated that approximately 18% of mixed-dentition patients had a transverse maxillary constriction,[12] which led to dentofacial deformities such as anterior deep overbite, posterior reverse overbite, and dental crowding. In general, the mid-palatal suture can be disrupted and separated by exerting a rapid transverse force on the maxillary dentition which surpasses the limit of orthodontic movement; continuous force increases cellular activity in the area and induces bone remodeling[13] in a process called rapid maxillary expansion (RME). Since mid-palatal suture opening was first reported by Angell, RME has become a widely performed procedure by orthodontists. RME is also considered crucial for remedying maxillary constriction in children and growing adolescents, as skeletal component rigidity limits expansion extent and stability as the patient matures. Some orthodontists suggest that early treatment to correct transverse discrepancy may avoid future extractions.[14] Of note, although the mid-palatal suture can be successfully opened, relapse of the posterior dentition width has been frequently reported;[15,16] forces that induce relapse continue to act for up to six weeks after active expansion.[17] A major reason for early relapse is inadequate bone formation in the suture. Consequently, a long retention period using a fixed retainer is often used to lessen the relapse. It was previously reported that the extent of relapse was related to the retention procedure after expansion, and thus a fixed retainer was required for at least two months.[18] However, the discomfort caused by the considerable volume of a fixed retainer may reduce patient self-discipline to maintain the effectiveness of a previous RME, and similarly, the fixed retainer may increase the risk of caries due to accumulated dental plaque. Therefore, many RME studies have focused on different approaches to enhance new bone formation, strengthen post-treatment width, ensure enough stability, and shorten the retention period.[19–23]

The pueraria plant is believed to be one of the earliest traditional herbs used in ancient Chinese medicine. Puerarin is a phytoestrogen first isolated from the pueraria root in the late 1950s and is one of the main isoflavone components in the root.[24] In 2005, the pueraria plant was identified as the 6th most important food crop by the World Food and Agriculture Organization. The pharmacological activity of puerarin has been extensively investigated since its isolation, with activities including neuroprotective effects,[25] vasodilatory activity,[26] cardioprotective activity,[27] anti-diabetic activity and the inhibition of diabetic complications,[28] anti-Parkinson's disease activity,[29] anti-Alzheimer's disease activity,[30] anti-osteoporotic activity,[31] antioxidant activity,[32] and others.[24] Furthermore, evidence has suggested that puerarin dissolved in collagen matrix increases new bone formation in bone graft defect sites and may be used for bone grafting and bone regeneration after surgery.[33,34] Therefore, it is reasonable to hypothesize that pueraria treatment may promote bone regeneration in the mid-palatal suture. As no reports on the puerarin stimulation of bone formation in the mid-palatal suture have been published, our objective was to investigate the effects of puerarin on osteogenesis in vitro and bone regeneration in vivo in the expanding mid-palatal suture and provide a theoretical foundation for its therapeutic effects toward RME and relapse prevention.

Materials and Methods
Isolation, Culture, and Verification of Cells

The study was complied with the ARRIVE guidelines and carried out in accordance with the UK Animals (Scientific Procedures) Act, 1986 and associated guidelines, EU Directive 2010/63/EU. The study was approved by the Animal Research Committee of School of Stomatology, Shandong University (Protocol No.: 20210121). All efforts were made to minimize the number of animals used and their suffering.

Rat bone marrow-derived mesenchymal stem cells (BMSCs) were accessed from bilateral femora and tibiae of two-week-old Wistar rats from the Laboratory Animal Center of Shandong University. Euthanized rats were soaked in and sterilized with 75% alcohol; bilateral femurs and tibiae were separated under aseptic conditions within 15 min to ensure the cell activity. After washing the long bones, the metaphyses were removed, and bone marrow was harvested out from

the cavity with α-minimum essential medium (α-MEM; Hyclone, Logan, UT, USA), complemented with 15% fetal bovine serum (FBS; Biological Industries, Israel) and 1% penicillin/streptomycin (Hyclone; GEHealthcare Life Sciences, Logan, UT, USA). BMSCs were collected after suspension and cultured in the incubator in a humidified atmosphere of 95% air and 5% CO2 at 37 °C, the medium was renewed every 3 days. Once the cells reached 80%, they were rinsed with phosphate-buffered saline (PBS), digested with a 0.25% trypsin-EDTA solution (Thermo Fisher Scientific Inc) and sub-cultured with complete medium. BMSCs at passage 3 were used in subsequent experiments. Eventually, the expressions of cell surface molecular markers (CD 34, CD 44, CD 45, and CD 90) were analyzed by flow cytometer (Beckman Coulter, Franklin Lakes, NJ, USA) to identify the stem cell properties of the collected BMSCs.

Osteogenic and Adipogenic Induction

To identify the multi-directional differentiation potential of BMSCs, they were induced by osteogenesis and adipogenesis. The cells in passage 3 were seeded in 6-well plates at a density of 1.0×10^5 cells per well and cultured to 90% confluence with complete medium, and then, the medium was changed to osteogenic inducing medium (α-MEM containing 8% FBS, 50 μg/mL ascorbic acid, 10 mM β-glycerophosphate and 0.01 μM dexamethasone) (Sigma-Aldrich) or adipogenic inducing medium (α-MEM containing 8% FBS, 500 μM 3-isobutyl-1-methylxanthine, 200 μM indomethacin, 1 μM dexamethasone and 10 μg/mL insulin) (Sigma-Aldrich). After culturing for 21 days, BMSCs were fixed with 4% paraformaldehyde, stained with Oil Red O and Alizarin Red S (Cyagen Bio-Sciences, Guangzhou, China).

Cell Proliferation Assay and Colony Formation Assay

The Cell-counting Kit-8 (CCK-8; Dojindo Laboratories, Kumamoto, Japan) was used to determine the effect of puerarin on the proliferation of BMSCs. BMSCs were placed in 96-well plates with complete medium at a density of 5000 cells per well for 24 h. Next, the medium was replaced by complete medium supplemented with puerarin (GN10680; GlpBio, American) (Figure 1A) at different concentrations (0, 10^{-3}, 10^{-4}, 10^{-5}, 10^{-6}, 10^{-7} and 10^{-8} mol/L), five duplicate wells were set for each concentration group. 1, 3, 5 day(s) later, the medium was aspirated, and then 100 μL of Cell-counting Kit-8 solution (α-MEM and CCK-8 reagent mixing in a ratio of 9 to 1) was added into every tested well. Wells containing 100 μL CCK-8 solution without seeding cells were used as blank control. The absorbance of samples was measured by a microplate reader (SPECTRAstar, Nano, BMG Labtech, Ortenberg, Germany) at 450 nm after incubation for 2 h at 37 °C in a darkroom.

To determine the ability of clone formation, BMSCs were seeded in 6-well plates at a density of 600 cells per well for 10 days, after fixing with 4% paraformaldehyde, cells were stained with crystal violet (Solarbio, Beijing, China). Cell colonies (clusters with 50 or more cells originated from the same cell) were counted to determine the ability of BMSCs to proliferate and form colonies.

Evaluation of ALP Activity

The ALP activity assay is widely used to estimate the early osteogenesis ability of stem cells. BMSCs were plated in 6-well plates at a density of 1.0×10^5 cells per well and treated with osteogenic inducing medium containing different concentrations of puerarin (0, 10^{-4}, 10^{-5}, 10^{-6} and 10^{-7} mol/L). After 7 and 14 days of induction, cells were rinsed three times with PBS and solubilized in the lysis solution (ripa buffer and PMSF mixing in a ratio of 99 to 1) (Solarbio, Beijing, China) for 15 min on ice. Lysed the collected solution under ultrasound for 10 cycles (Bioruptor Pico, Diagenode, Belgium), and then, cell lysates were centrifuged at 12,000 × g for 5 min at 4 °C. The supernatant was collected to obtain protein. Following the instructions of the manufacturer, an ALP activity assay kit (Nanjing Jiancheng Bioengineering Institute, Nanjing, China) was used to measure the absorbance of the samples using a microplate reader at 520 nm. ALP activity was normalized to the respective total protein concentration detected by the bicinchoninic acid (BCA) protein assay kit (Solarbio, Beijing, China).

Alizarin Red S Staining

BMSCs were plated in 6-well plates at a density of 10^5 cells per well and treated with osteogenic inducing medium containing different concentrations of puerarin (0, 10^{-4}, 10^{-5}, 10^{-6} and 10^{-7} mol/L) for 21 days. After fixed with 4%
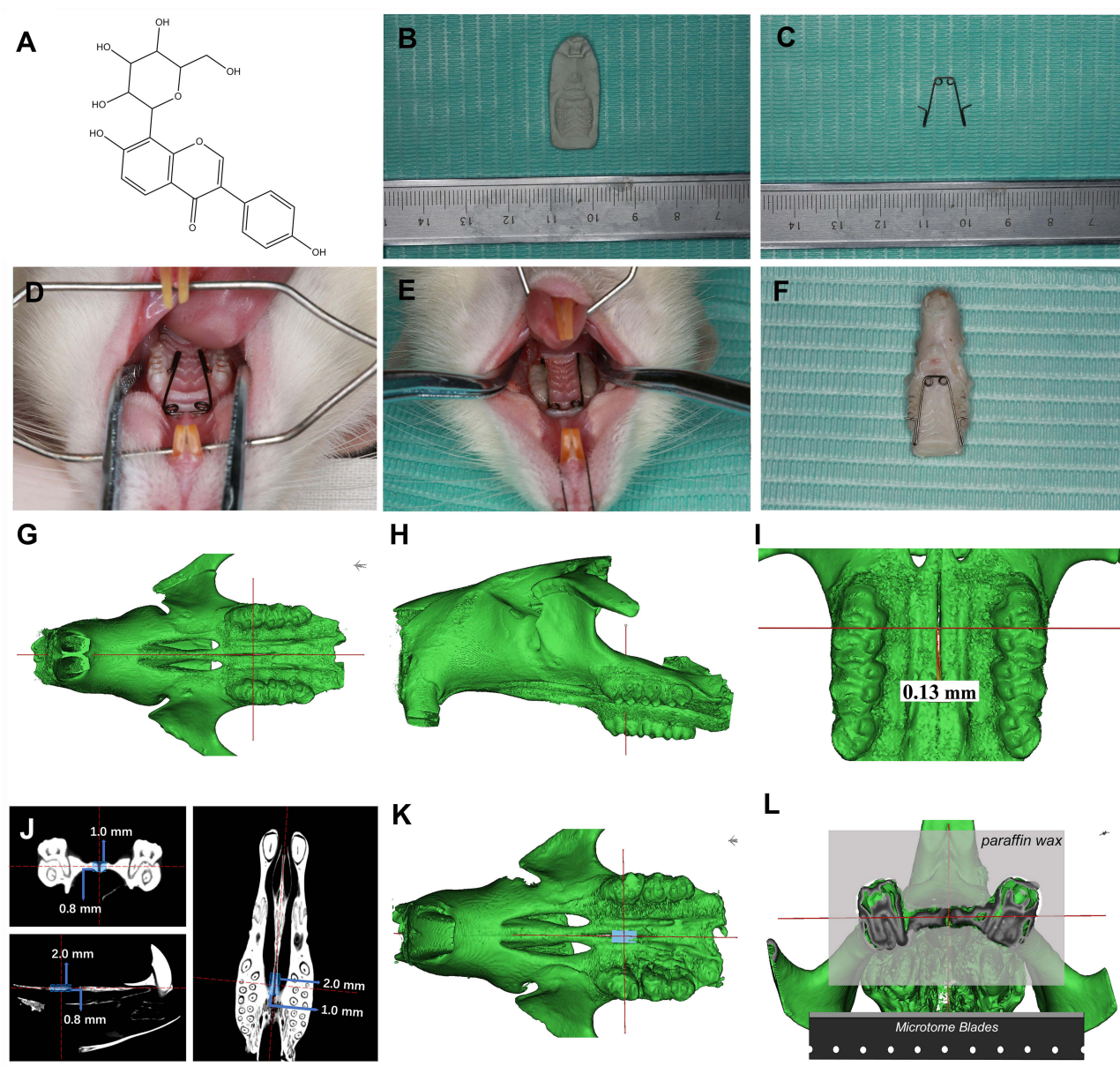
Figure 1 Model of rapid maxillary expansion (RME) and three-dimensional reconstruction of the occlusal view of the rat maxilla. (**A**) Chemical Structure of Puerarin (C21H20O10). (**B**) Plaster model of rat maxillary. (**C**) Expansion appliance. (**D**) Inserted expansion appliance. (**E**) Bonded expansion appliance. (**F**) Rat maxillae after carefully dissected. (**G**) Rat head in the occlusal view, the vertical red line marking the occlusal position of the mid-coronal plane of the upper first molar, the horizontal red line marking the position of mid-palatal suture. (**H**) Rat head in the sagittal view, the red line marking the sagittal position of the mid-coronal plane of the upper first molar. (**I**) The distance of the mid-palatal suture in one of the rats in group 1 is 0.13mm. (**J**) The position and length of the ROI (2.0mm*1.0mm*0.8mm) in the coronal plane, horizontal plane, sagittal plane respectively. (**K**) 3D position view of ROI. (**L**) Location and plane of sectioning in the mid-palatal region.

paraformaldehyde for 30 min, cells were stained with Alizarin red S (pH 4.1, Sigma-Aldrich) for 15 min, the stained plates were scanned to evaluate mineralized matrix deposition. Then, 10% cetylpyridinium chloride (CPC; Solarbio, Beijing, China) was added to the stained plates to dissolve the mineral nodules. The absorbance of the solution used to quantify the mineral nodules was measured by a microplate reader at 562 nm.

RNA Extraction and Real-Time PCR Analysis of BMSCs

BMSCs were cultured in osteogenic inducing medium containing different concentrations of puerarin (0, 10^{-5}, 10^{-6} mol/L) for 7 and 14 days. According to the manufacturer's instructions, the Evo M-MLV RT Kit with gDNA Clean for qPCR II (AG11711; Accurate Biology, Hunan, China) was used to isolate total mRNA and prepare cDNA. The SYBR® Green

Premix Pro Taq HS qPCR Kit (AG11701; Accurate Biology, Hunan, China) and a Roche Light Cycler® 480 Sequence Detection System (Roche Diagnostics GmbH, Mannheim, Germany) were used to perform reverse transcriptase polymerase chain reaction (RT-PCR), and a reaction system of 10 μL volume was adopted. Every RNA sample was tested in triplicate, and each experiment was repeated at least 3 times, the mRNA expression levels were calculated by the $2^{-\Delta\Delta Ct}$ method using *glyceraldehyde-3-phosphate dehydrogenase (GAPDH)* as a control. The primer sequences used in the present study were as follows: *ALP (+)*: 5′-AGTGTGGCAGTGGTATTGTAGG-3′ and 5′-CACACACAAAGCACTCGGGG-3′; *SP7 (-)*: 5′- GGT CCTGGCAACACTCCTAC-3′ and 5′-AAGAGGTGGGGTGCTGGATA-3′; *BSP (-)*: 5′-AGCTGACCAGTTATGGCACC -3′ and 5′-TTCCCCATACTCAACCGTGC-3′; *OCN (+)*: 5′-TGACAAAGCCTTCATGTCCAAG-3′ and 5′-GAAGCC AATGTGGTCCGCTA-3′; *GAPDH (+)*: 5′- ACTCCCATTCTTCCACCTTT-3′ and 5′-CCCTGTTGCTGTAGCCATATT -3′. The plus sign (+) indicates that the primers cross exon boundaries.

Western Blot Analysis

After culturing in osteogenic inducing medium containing different concentrations of puerarin (0 and 10^{-5} mol/L) for 14 days, BMSCs were lysed with RIPA lysis buffer containing 1% PMSF (Solarbio, Beijing, China). The total collected protein concentrations were quantified by a BCA protein assay kit. All protein samples (20μg) were denatured and separated via 10% sodium dodecyl sulfate-polyacrylamide gel electrophoresis (SDS-PAGE) and were transferred onto 0.45-μm polyvinylidene difluoride membranes (PVDF; Millipore, Billerica, MA, USA). Afterwards, the membranes were blocked with 5% skimmed milk at room temperature for 1 h and incubated with primary antibodies that recognized β-catenin (1:800; Cell Signaling Technology, Danvers, MA, USA), GAPDH, ALP, Runx2, Collagen I (Col I) (1:1000; Abcam, Cambridge, MA, USA) overnight at 4 °C. After washing in Tris-buffered saline with 0.1% Tween 20 (TBST), the membranes were incubated with a secondary antibody (Absin, Shanghai, China) solution at 37 °C for 1 h. Secondary antibodies were selected based on the source of primary antibodies. An enhanced chemiluminescent substrate kit (Millipore) and a chemical imaging system (Amersham Imager 600; GE Healthcare, Little Chalfont, UK) were used to detect immunoreactive proteins. GAPDH was used as internal reference.

Animal Experimental Design and Appliance Placement

The rats were pair-housed in standard plastic cages in a specific pathogen-free animal laboratory of School of Stomatology, Shandong University, under controlled temperature (22 ± 1°C), humidity (55 ± 10%), interior noise (below 60dB) and a 12-h light/dark cycle. They were provided with a powder diet and water ad libitum. All the animals were acclimated for 1 week before the experiment started. The general condition and weight of each rat were monitored daily during the experiment.

Eighteen 6-weeks-old male Wistar rats (mean weight 200~220 g) were adopted in the present research. The animals were randomly divided into three groups as follows: group 1, six control rats without any treatment; group 2, six rats received rapid maxillary expansion and saline solution (15mg/kg/day) containing 2% DMSO; group 3, six rats received rapid maxillary expansion and puerarin (15mg/kg/day) dissolved in 2% DMSO and then diluted with saline. Based on the width of the dental arch from the rat maxillary plaster model (Figure 1B), a 0.014-inch Australian wire (TP Original Premier Wire, TP Orthodontic Appliance Co. Ltd, Wuxi, China) was used to bend the expansion appliances with two helices and two arms (Figure 1C). Rats in groups 2 and 3 are anesthetized by an intramuscular injection of 3 mg/kg xylazine hydrochloride and 35mg/kg ketamine hydrochloride to ensure the smooth progress of the maxillary expansion surgery. After calibrating the expansion force between the two arms to 100 ± 5g, the appliance was inserted into the bilateral first and second maxillary molars (Figure 1D) and the stability of the RME system was enhanced with the addition of light-cured adhesives (Gluma Comfort Bond, Heraeus Kulzer GmbH, Hanau, Germany) (Figure 1E). The injection solution of puerarin was freshly prepared by solubilizing in 2% dimethyl sulfoxide (DMSO) before diluted in saline, and it must be applied within 15 min in the case of puerarin precipitate. The injection sites were located in the space between the frontal periosteum and the maxillary suture, and a disposable sterile insulin syringe with a 29G, 0.33*13 mm needle (Kindly Medical Devices, Shanghai, China) was used to minimize tissue damage. On day 14 after installation, all animals were generally anesthetized and then perfused transcardially with 4% paraformaldehyde (pH

7.2~7.6) for fixing, and their maxillae were carefully dissected (Figure 1F) for micro-CT analyses and histological examinations.

Micro-CT Scanning of the Hard Palate

The maxillae of the rats were scanned using high-resolution scan mode (Quantum GX2 micro-CT, PerkinElmer, American) at the condition of 90 kV and 88 μA, the 72*72mm FOVs was chosen with an effective pixel size of 9.0 μm. The digital image was analyzed with Materialise's interactive medical image control system V20.0 (MIMICS V20.0) and its accompanying software 3-MATIC. We imported the scanned data from micro-CT into MIMICS to build a 3D model of rat and placed the maxillary bones in the same orientation by calibrating the red reference line on the figure (Figure 1G and H). The width of the mid-palatal suture was obtained by measuring the expanded distance at the level of the mid-coronal plane of the upper first molar (Figure 1I). Meanwhile, the region of interest (ROI) (2.0mm*1.0mm*0.8mm) builded through 3-MATIC included the mid-palatal suture and the bilateral bone, the position of the ROI was shifted to ensure that the intersection of the red dotted lines (Figure 1J) was in the center of the ROI (Figure 1K). The osteogenesis ability of puerarin during RME was investigated by measuring the changes of the bone volume in ROI.

Histological Examination

The specimens were decalcified in 10% ethylenediaminetetraacetic acid/phosphate-buffered saline for 8 weeks, then dehydrated through the ethanol series, rendered transparent by xylene, embedded in paraffin wax. Serial sections with a thickness of 5 μm were prepared through bilateral maxillary first molars on the coronal plane (Figure 1L). Hematoxylin and eosin (HE) staining and Masson staining for histologic observation were performed following manufacturer's instruction.

Immunohistochemical Staining

Sections were dewaxed in xylene and rehydrated in graded ethanol baths, then enzyme-treated with 0.1% (w/v) trypsin at 37 °C for 10 min to antigen retrieval, blocked with 3% hydrogen peroxidase for 30 min to inhibit endogenous peroxidase activity, preincubated in normal goat serum for 35 min to blocked nonspecific binding. Next, we incubated rabbit polyclonal antibody (Abcam Inc., MA, USA) against BMP2 (working dilution, 1:200) and ALP (working dilution, 1:150) in humid chamber overnight. Subsequently, sections were rinsed in PBS, and the immune reaction was detected according to the 2-step DAB detection kit (Zhongshan Golden Bridge Biotechnology, Beijing, China). All sections were counterstained with hematoxylin for 3 min, followed by running water for 10 min. Under 400 × magnification, the average optical density (AOD) value of the immunohistochemical images was analyzed by ImageJ (National Institutes of Health). The process was performed in five randomly selected visual fields per animal, and the average values were calculated by one person repeating at least three times.

Statistical Analysis

All data were obtained from at least three replicates of each experiment. Statistical analyses were performed with GraphPad Prism 8 (GraphPad Software Inc., La Jolla, CA, USA) and Microsoft Excel 2020 (Microsoft Corporation, Redmond, WA, USA). A one-way or two-way analysis of variance (ANOVA) was performed to analyze statistical calculations. All the above results were shown as the means ± standard deviation. All data were considered statistically significant when $P < 0.05$.

Results
Isolation and Characterization of Rat BMSCs

Rat BMSCs were harvested, purified, and cultured through the whole bone marrow wall-adherence method in vitro. Generally, primary BMSCs exhibited colony growth after 3~5 days with a typical long-spindle-like and a number of protruding formations (Figure 2A). After 3 or more passages in culture, they tended to be more morphologically
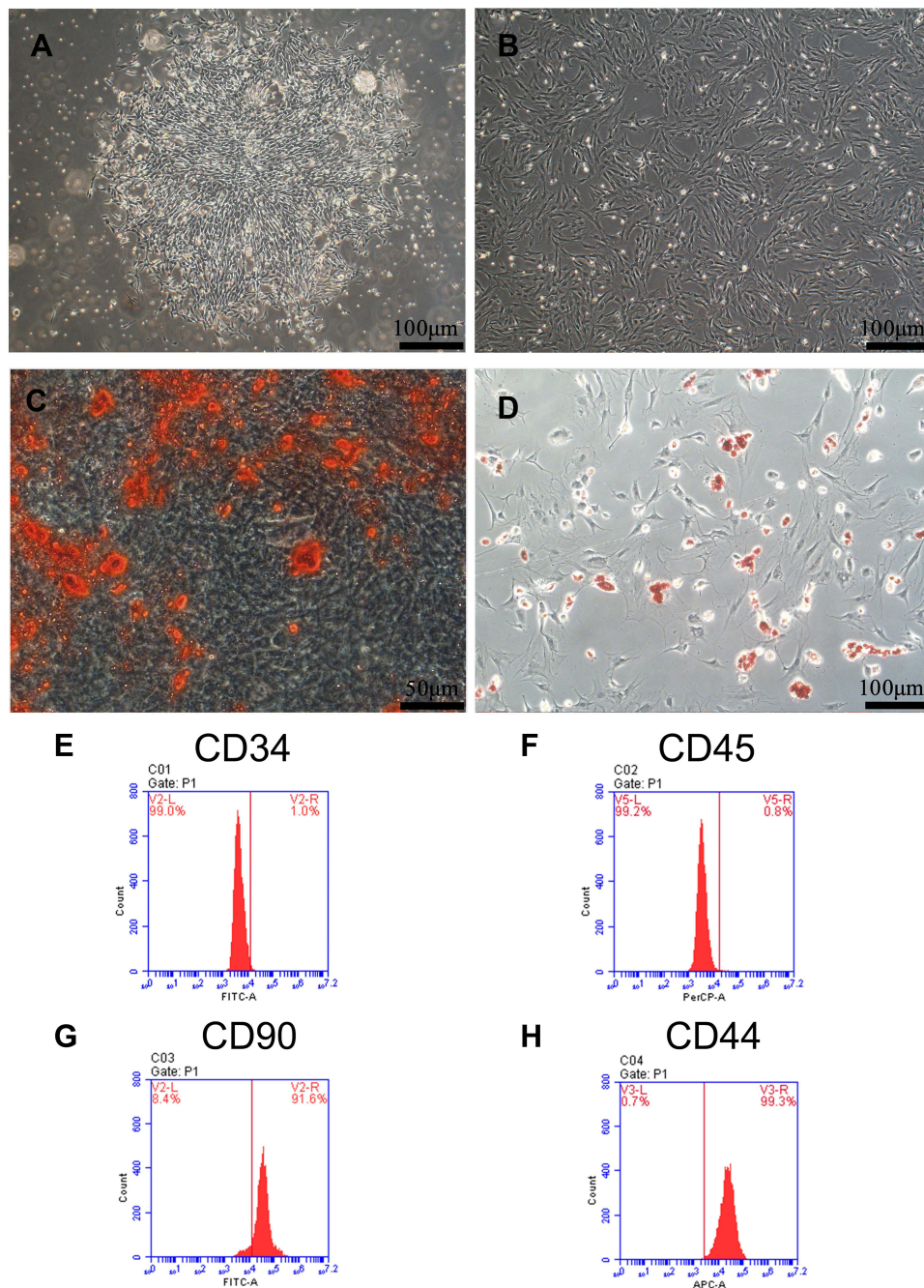
Figure 2 Cultivation and characterization of BMSCs. (**A**) Cell morphology of primary BMSCs. Scale bar: 100 μm. (**B**) Cell morphology of passage 3 BMSCs. Scale bar: 100 μm. (**C**) BMSCs were stained with Alizarin red S after osteogenic differentiation induction. Scale bar: 50 μm. (**D**) BMSCs were stained with oil red O after adipogenic induction. Scale bar: 100 μm. (**E–H**) Analysis of BMSCs surface markers expression by flow cytometry. The high expression is on the right side of the central axis. The expression of CD34 and CD45 were negative, while CD90 and CD44 were highly expressed.

heterogeneous (Figure 2B). Following 3 weeks of osteogenic and adipogenic induction, the formation of Alizarin Red mineralized nodules showed the osteogenic potential of BMSCs (Figure 2C), and the Oil Red O lipid droplets indicated their adipogenic potential (Figure 2D). Furthermore, flow cytometry analysis was performed to identify the phenotypic characteristics of these mesenchymal stem cells (MSC). The results showed that BMSCs had high expression of MSC-specific markers CD44 and CD90 but negative for CD34 and CD45 (Figure 2E–H). Collectively, the above conclusions indicated that the isolated adherent cells were phenotypically and functionally equivalent to typical MSCs.

Effect of Puerarin on Proliferation and Colony Formation of BMSCs

The results of the cell proliferation are analyzed by the CCK-8 assay (Figure 3A and B). On day 3, compared with the control group, proliferative capacity of BMSCs at the puerarin concentrations of 10^{-6} mol/L was significantly higher (P < 0.01), the 10^{-4}, 10^{-5} and 10^{-7} mol/L group also showed a clear increase (P < 0.05), the 10^{-8} mol/L group showed a slight increase, but there was no statistically significant (P > 0.05). As time gone by, the trend of the effect of puerarin on proliferation of BMSCs became pronounced. Conversely, the 10^{-3} mol/L group markedly inhibited the proliferation of BMSCs (P < 0.0001). Considering the cytotoxic effects, 10^{-4}, 10^{-5}, 10^{-6} and 10^{-7} mol/L groups were chosen for the following assays. The colony formation assay showed that after culturing for 10 days, the cell colonies of the 10^{-6} mol/L group were obviously larger and more numerous (P < 0.01) than those of the control group (Figure 3C–E).

Effects of Puerarin on the Osteogenic Differentiation of BMSCs

This research measured the ALP activity level of BMSCs cultured with different concentrations of puerarin (0, 10^{-4}, 10^{-5}, 10^{-6} and 10^{-7} mol/) in two periods (Figure 4A). It was found that compared with the control group, ALP activity level at the various concentrations of puerarin measurably increased to different degrees (P < 0.05) on day 7 and day 14 with the similar trend; clearly, 10^{-6} mol/L group obtained the best effects. For the alizarin red S staining assay (Figure 4B–E), the 10^{-6} mol/L
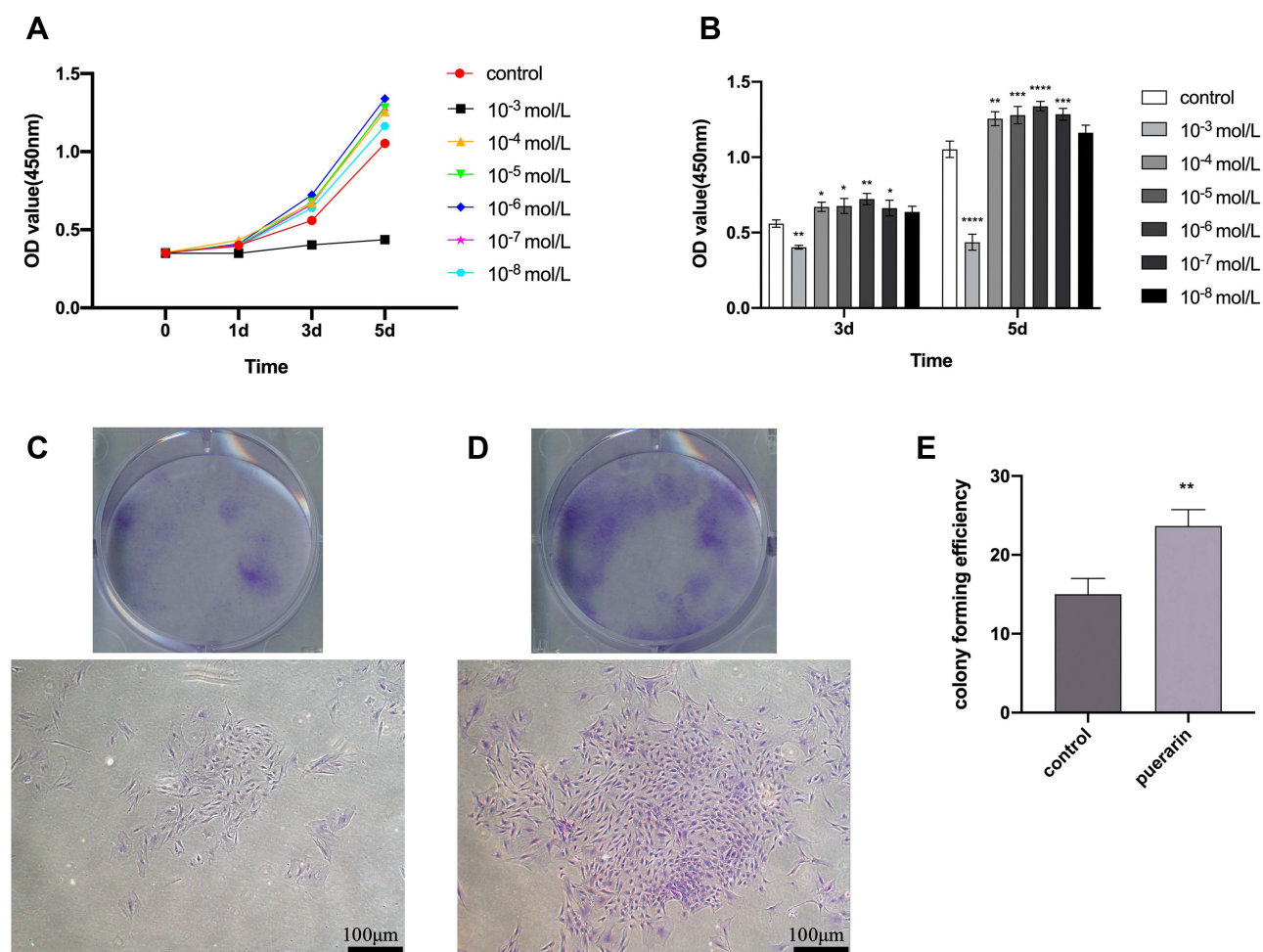

Figure 3 Effects of puerarin on the proliferation of BMSCs. (**A**) The growth curves of puerarin-treated groups at different concentration were drawn according to the results of CCK-8 analysis. (**B**) CCK-8 analysis for the proliferation of BMSCs in various concentration of puerarin on day 3 and 5 (two-way analysis of variance). (**C** and **D**) Colony formation assay was performed to test the colony forming capacity of BMSCs. After 10 days, more and larger cell colonies were observed in the experimental group (**D**) than those in the control group (**C**). (**E**) The colony forming efficiency of 10^{-6} mol/L puerarin group (one-way analysis of variance). Scale bar: 100 μm. The columns represent the means. Error bars represent standard deviations. *P< 0.05, **P < 0.01, ***P < 0.001, ****P < 0.0001.
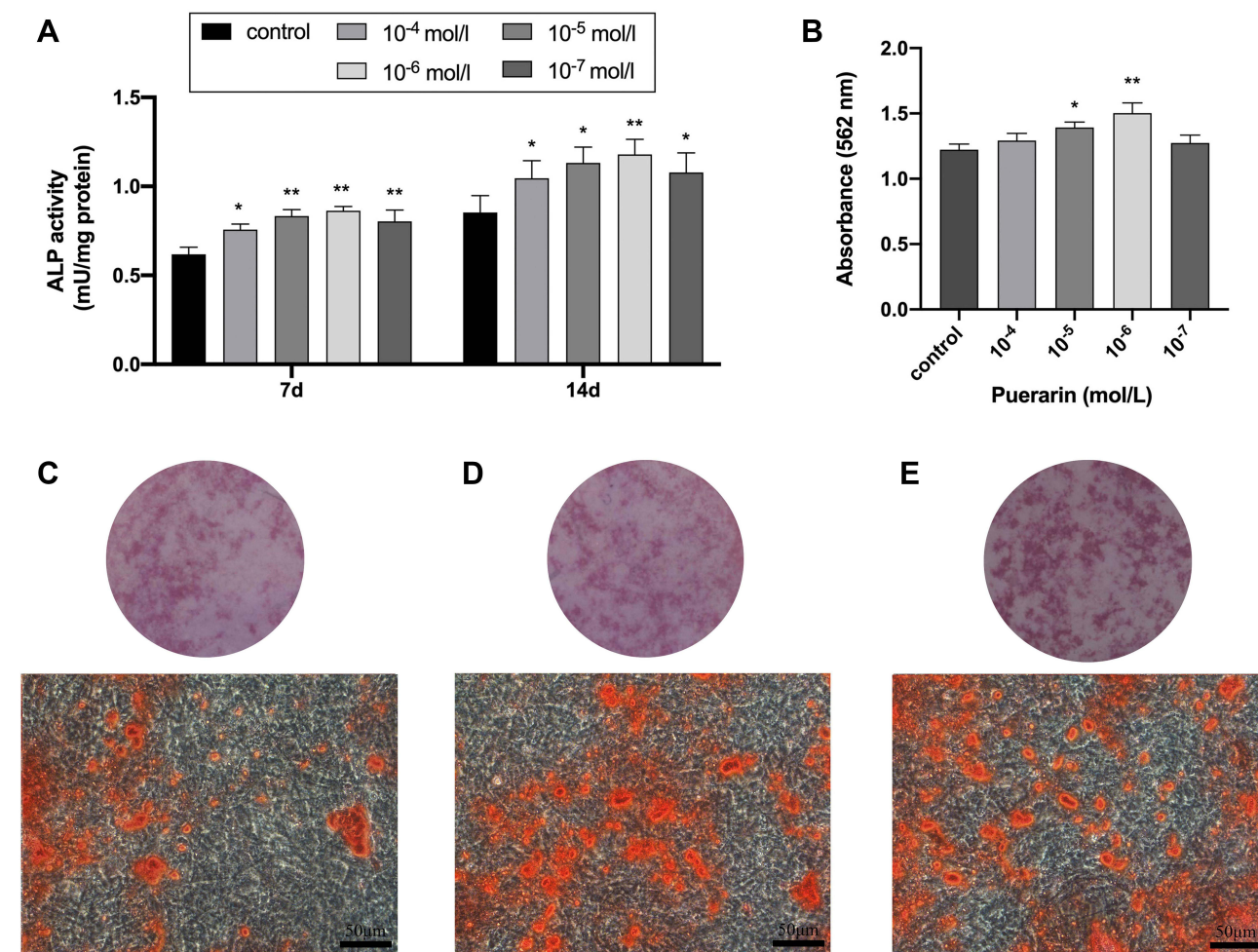
Figure 4 Effects of puerarin on ALP activity and mineralized nodule deposition of BMSCs. (**A**) ALP activity quantification of BMSCs stimulated with puerarin for 7 and 14 days (two-way analysis of variance). (**B**) Quantitative analysis of Alizarin red S staining of BMSCs stimulated with puerarin for 4 weeks (one-way analysis of variance). (**C–E**) Alizarin red S staining of control group (**C**), 10^{-5} mol/L (**D**) and 10^{-6} mol/L (**E**) puerarin group. Scale bar: 200 μm. The columns represent the means. Error bars represent standard deviations. *$P < 0.05$, **$P < 0.01$.

group showed the strongest capacity of matrix mineralization ($P < 0.01$), more and larger calcified nodules were observed in the 10^{-5} and 10^{-6} mol/L groups. Based on the above measurements, we conclude that 10^{-6} mol/L is the optimal concentration for the proliferation and osteogenesis of BMSCs. Besides, it is worth noting that 10^{-5} mol/L has the same positive effect on BMSCs which is only slightly weaker than the optimal concentration, so the concentrations of 10^{-5} and 10^{-6} mol/L were used in the real-time PCR analysis to enhance the reliability of the experiment, and the concentrations of 10^{-6} were used in the Western blot analysis. The mRNA expression levels of the osteogenesis-related genes (*ALP, SP7, BSP* and *OCN) and the protein expression levels of the* osteogenesis-related proteins (Col I, β-catenin, Runx2, and ALP) were evaluated to assess the osteogenic promotion effect of puerarin. Compared with the control group, the two puerarin-treated group significantly enhanced the expression of the above-mentioned genes on day 7 and day 14 ($P < 0.05$; Figure 5A–D). Furthermore, compared to the control group, the protein expression levels of Col I, β-catenin, ALP, Runx2 were showed an upregulated trend on day 14 (Figure 5E). These data indicated that puerarin might play a positive role in the osteogenic differentiation of BMSCs.

Changes in Body Weight and Mid-Palatal Suture Widths

The body weights decreased of the rats in group 2 and group 3 at day 1~5, due to the initial in adaptation to the maxillary expansion appliances, which were significantly different from the steady increase in group 1 ($P < 0.05$; Figure 6A). However, from day 6, the weight gradually gained among all rats with no significant differences. In addition, there is no
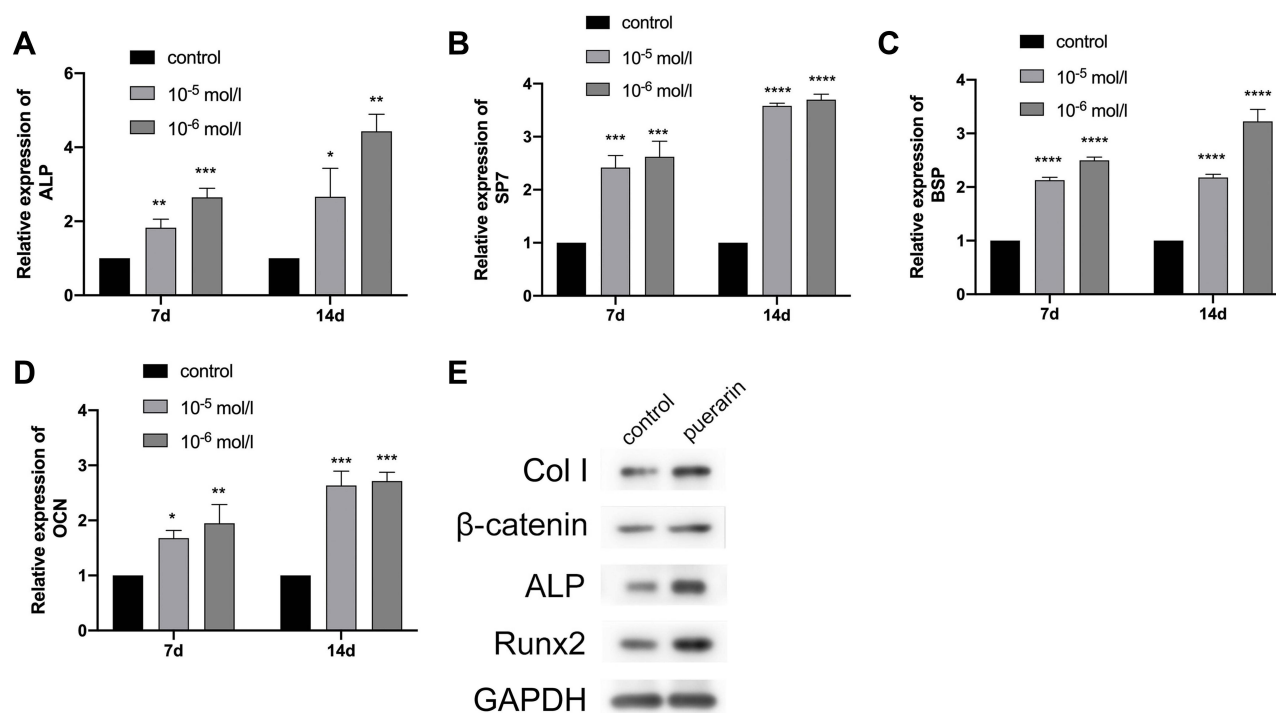
Figure 5 Effect of puerarin on the *ALP* (**A**), *BSP* (**B**), *OCN* (**C**), *SP7* (**D**) expression of BMSCs at 7 and 14 days (two-way analysis of variance). The mRNA expression level of GAPDH was used as internal reference. The columns represent the means. Error bars represent standard deviations. *P < 0.05, **P < 0.01, ***P < 0.001, ****P < 0.0001.
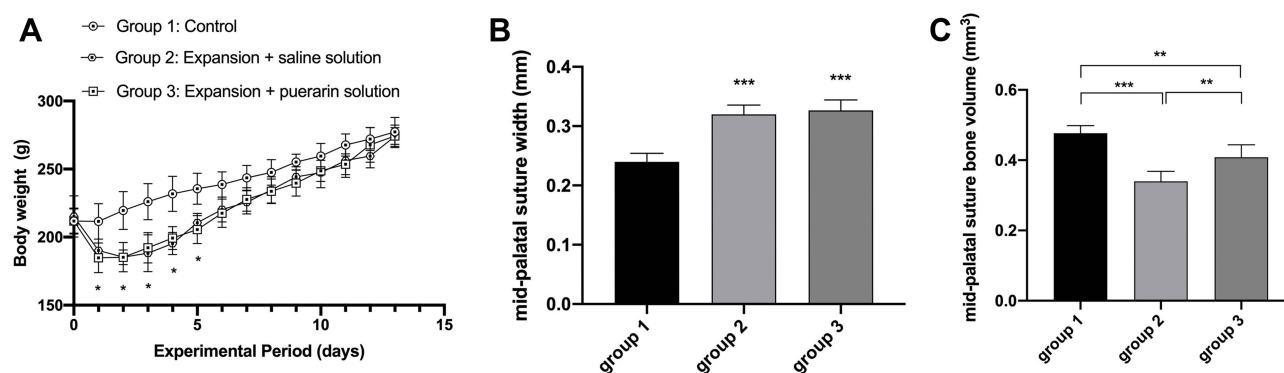

Figure 6 Animal weight and changes of mid-palatal suture response to the expansion force (n=6). (**A**) Changes of body weight during experimental period (two-way analysis of variance). (**B**) Width of the mid-palatal suture (one-way analysis of variance). (**C**) Bone volume of the mid-palatal suture (one-way analysis of variance). The columns represent the means. Error bars represent standard deviations. *P < 0.05, **P < 0.01, ***P < 0.001.

significant difference in weight between group 2 and group 3 during the study (P > 0.05). The results showed that the rats recovered quickly from the surgery and were well tolerated to the experimental condition. Micro-CT analysis revealed that compared with group 1, the mid-palatal sutures of rats in groups 2 and 3 were expanded after expansion surgery at day 14 (P < 0.01; Figure 6B), indicating that the RME animal models were successfully established. However, there was no statistical significance (P > 0.05) between group 2 and 3 in terms of the expanded width of the mid-palatal suture. The data of bone volume in the fixed region was measured for evaluating new bone formation in the mid-palatal suture. Compared with group 1, the bone volume in groups 2 and 3 showed significantly reduce (P < 0.01; Figure 6C). Moreover, the bone volume in group 3 was higher than that in group 2 (P < 0.01), implied the application of puerarin had a positive effect on mid-palatal suture osteogenesis.

Histological Alteration in the Mid-Palatal Sutures

HE-stained (Figure 7A–C) showed the mid-palatal suture in rat of group 1 is made up of a thin band cellular fibrous tissue in the middle and bilateral cartilage with chondrocytes covering the edges of palatal bones. After the mechanical stimulation, the width of the mid-palatal suture is significantly enlarged in response to external force, and two layers of secondary cartilage expand towards the reddish widened fibrous tissue following the same direction as the expansive force, concomitant with the chondrocytes proliferated and differentiated into hypertrophic chondrocytes. Masson staining (Figure 7D–F) showed that the cartilage and the collagen fibers in the area of the expanded mid-palatal suture were stained blue, and more hypertrophic chondrocytes were found in group 3 compared with group 2, implying more active endochondral ossification was in progress in group 3.

Immunohistochemistry Analyses for BMP2 and ALP

The positive expressions for osteogenic markers ALP (Figure 7G–I) and BMP2 (Figure 7J–L) were the brownish-yellow stained particles that were mainly observed in the osteoblasts, chondrocytes and fibrous tissue around the mid-palatal suture. Low expression level of ALP and BMP2 was detected in the mid-palatal suture of group 1 accompanied by the absence of few positive cells, while strong signals of them were observed around the expanded suture in group 2 and group 3 which possess the characteristics of big volume and abundant amount of the positive cells, implying active new bone formation in the mid-palatal suture region. Furthermore, compared with group 2, more intense expression was recognized in group 3 according to the higher AOD value ($P < 0.01$; Figure 7M and N).

Discussion

Our data suggested that puerarin upregulated the proliferation and osteogenic differentiation of BMSCs. Also, the local administration of puerarin enhanced new bone formation in our RME rat model. RME is a distraction osteogenesis (DO) surgical technique that generates new bone between separated bone segments via the application of continuous and stable force. The procedure is advantageous in terms of low surgical trauma, no requirements for bone grafting, and peripheral soft tissue can be expanded at the same time. Since its first introduction in 1969,[35] the DO technique has been widely used to enhance bone regeneration in orthopedic and oral/maxillofacial disorders.[36] However, a limitation of RME is that newly formed immature bone tissue requires a prolonged consolidation period to mature, mineralize, and achieve desired distances, which may sometimes trigger oral complications or be often ignored by patients. To ensure its therapeutic efficacy, numerous methods have been investigated, including low-power laser therapy,[19] LED (light-emitting diode) phototherapy,[37] vitamin supplementation,[20] isoquercitrin administration,[21] sex steroids,[22] curcumin and melatonin,[23] and strontium ranelate.[38]

Based on the data from in vitro and in vivo studies, puerarin was effective in inhibiting bone resorption and improving bone structure. Previous studies showed puerarin decreased receptor activator of nuclear factor κ-B ligand (RANKL) expression and increased osteoprotegerin (OPG) expression to stimulate osteoblastic proliferation,[39] which induced the upregulation of miR-155-3p,[33] BMP2 expression and nitric oxide (NO) synthesis[40] to promote cell differentiation and bone formation. Furthermore, puerarin can promote osteogenic differentiation which involved ERK1/2 and p38-MAPK pathway,[41] ER, p38 MAPK, and Wnt/β-catenin pathways,[42] and PI3K/Akt pathway.[43] Also, puerarin prevented osteoclastogenesis by inhibiting Akt activation in RAW264.7 cells[44] and blocking monocyte chemotactic protein-1 (MCP-1) production.[45] In our study, puerarin dose-dependently enhanced osteogenic differentiation and mineralization, and upregulated *ALP, SP7, BSP* and *OCN* mRNA levels, suggesting positive stimulatory effects on osteogenic differentiation. Moreover, increased ALP activity after treatment with puerarin was observed in other studies[46] in agreement with our findings. *ALP* has important roles in osteoid formation and mineralization,[46] therefore ALP activity is an early osteoblast differentiation marker; *BSP* is a phosphorylated glycoprotein mainly expressed in mineralized tissue such as bone, and was shown to be the main synthetic product of active osteoblasts;[47] *OCN* is an important component in bone endocrinology and is secreted solely by osteoblasts;[48] and *SP7* is a critical regulator of osteoblast differentiation and bone formation and induces pre-osteoblast differentiation into fully functional osteoblasts.[49] A lot of growth factors, hormones and proteins participate in osteoblast differentiation of MSCs. The Wnt/β-catenin
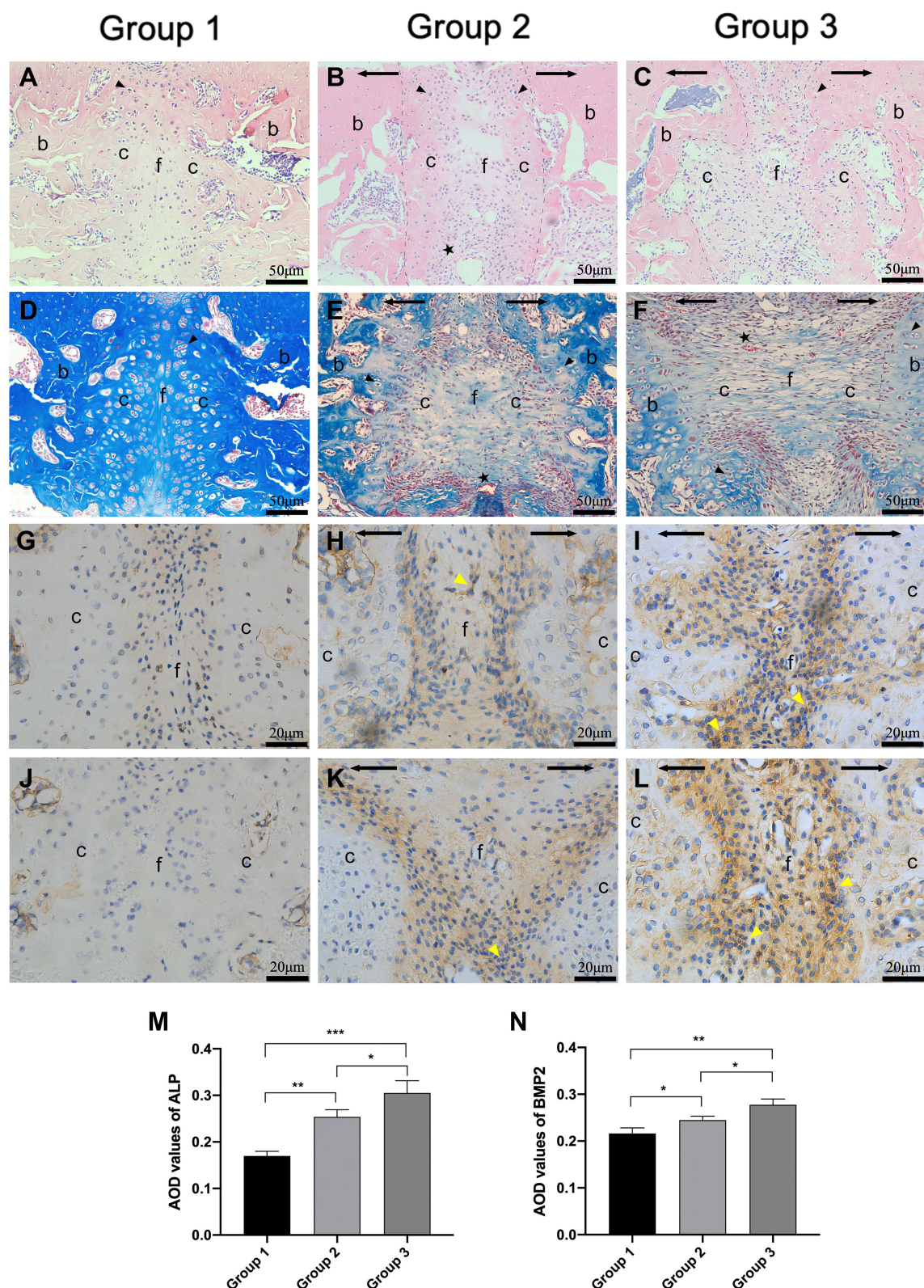
Figure 7 Histological alterations and immunohistochemistry analyses in the mid-palatal sutures. (**A–C**) HE staining showed the changes of the mid-palatal suture in histological sections. (**D–F**) Masson staining showed the changes of the mid-palatal suture in histological sections. b, maxillary bone; c, cartilage; f, fibrous tissue; black arrow: the direction of stretch force; black triangle: the chondrocyte; black pentagram: the capillary; black dotted line: expanded region. Scale bar: 50 μm. (**G–I**) ALP was detected by immunohistochemistry analyses. (**J–L**) BMP2 was detected by immunohistochemistry analyses. Yellow triangle: the positive signal. Scale bar: 20 μm. (**M** and **N**) Quantification of the expression level of ALP and BMP2 (one-way analysis of variance). The columns represent the means. Error bars represent standard deviations. *P < 0.05, **P < 0.01, ***P < 0.001.

signaling pathway is known as one of the important and typical molecular cascades that regulate osteogenic throughout lifespan. Studies have shown that activation of Wnt/β-catenin pathway promotes BMSC osteogenic differentiation and osteogenesis.[50,51] The protein β-catenin is the central target and an essential component of the Wnt/β-catenin signaling pathway.[52] β-catenin also can preserve the stem state of BMSCs through activation of EZH2.[53] Collagen type I (Col I), a protein abundantly found in the extracellular matrix, has been broadly shown to promote proliferation, survival, adhesion and osteogenesis in bone marrow MSCs.[54] There is evidence that Col I promotes osteogenic differentiation of amniotic membrane-derived mesenchymal stromal cells in basal and induction media.[55] It has been reported that growth on a remodeled Col I matrix by MMP13 stimulates osteogenic differentiation and self-healing of bone tissue via an MMP13/ITGA3/RUNX2 positive feedback loop.[56] Runx2 is a key transcriptional modulator for osteoblast differentiation that plays a fundamental role in osteoblast maturation and homeostasis;[57] it is considered as the master osteoblast-specific transcription factor even if many other factors coordinate bone remodeling. It is crucial in regulating bone differentiation of MSCs and is a key protein for bone formation.[58,59] Due to the vital role of MSCs in osteogenic differentiation, we conclude from the above study that puerarin can promote bone regeneration in vitro. Furthermore, the optimal puerarin concentration for BMSC proliferation and osteogenesis was 10^{-6} mol/L.

Several animal models, including cynomolgus monkeys, miniature pigs, beagles, rabbits, and rats have been used to study bone regeneration; however, the rat model is widespread due to low costs, wide access to animals, simple model operation, and minimally invasive procedures. The fall-off rate for expansion devices during rat studies is relatively low, which in turn decreases experimental steps and ensures the accuracy of experimental results. This model is similar to clinical RME, using bilateral maxillary first molar as the anchorage teeth, and the mid-palatal suture separated accompanied by the buccal movement of the bilateral maxillary first molar. A previous study reported that the ideal time for RME was the prepubertal or pubertal period, as ongoing growth and development usually generated more stable orthopedic results,[22] therefore 6-week-old rats were selected for this study. The experimental period was designed for 14 days. On the one hand, there would be a greater likelihood that the orthodontic force would decay to the point that it would not provide sufficient expansion of the mid-palatal suture after 2 weeks, thus, continuing the experiment may have less effect on the results. On the other hand, studies have shown that 7 and 10 days of RME already allow for an effective expansion of the mid-palatal suture.[21,38] As it is medically unethical to systemically administer extrinsic medicines to growing healthy patients, we used local injections to minimize adverse systemic effects and support bone formation at regular time intervals in a particular area of rats in this study. Moreover, assessing direct responses to puerarin in mid-palatal suture bone formation may limit its systemic-administration due to the aforementioned multiple puerarin interactions with various organs or tissues. To the best of our knowledge, ours is the first study to investigate the effects of this locally administered traditional herb and observe no degenerative changes around injection sites.

In recent years, micro-computed tomography has rapidly gained recognition as a standard scanning and analytical tool for bone structures due to its ability to gather key bone structural parameters, and accurately visualize structures in three dimensions.[60] In our study, the expanded distance of the mid-palatal suture was wider in groups 2 and 3 when compared with group 1, demonstrating a significant efficacy for RME in rats, in agreement with a previous study.[21] However, we observed no significant differences between groups 2 and 3 in terms of the expanded width of the mid-palatal suture, probably because DO can be divided into three temporal phases: a latency period of 5–10 days, a distraction phase, and a consolidation phase. The mid-palatal suture was in the early stage of distraction at day 14, forming a central fibrous zone as the primitive callus was stretched; this phase was rich in chondrocyte-like cells, fibroblasts, and oval cells which were morphological intermediates between fibroblasts and chondrocytes.[61,62] At this time, the puerarin effects on bone remodeling were at initial microscopic stages and were not yet reflected at the macroscopic level. Notably, a significant increase in bone volume was identified in group 3 in the expanded mid-palatal suture, suggesting accelerated new bone deposition and formation in response to puerarin.

Our immunohistochemical analyses showed that BMP2 and ALP expression increased in the expanded mid-palatal suture. BMPs are growth factors which belong to the transforming growth factor-superfamily; they induce endochondral bone formation[63] and are involved in bone regeneration during osteoblast differentiation, and their increased expression enhances new bone formation.[64] Similarly, ALP is a reliable biochemical marker of bone formation.[65] The AOD value showed puerarin increased ALP and BMP2 expression levels during RME, thereby upregulating bone regeneration.

Heterotopic ossification (HO) is one of the hot spots of research on post-traumatic complications,[66,67] and it has been reported that elevated BMP2 is positively correlated with the occurrence of HO.[68] It is noteworthy that though puerarin upregulates BMP2 level when it is used to stimulate osteogenesis in mid-palatal suture, we presume that HO is less likely to occur in the context of safe, physiological, controlled RME. The limitation of the study was that the precise osteogenic mechanism of puerarin towards BMSCs was not fully elucidated as RME is a complex process; the effect of puerarin on osteoblast differentiation is an area worthy of further exploration, therefore future research must elucidate more biological effects of puerarin on bone regeneration.

Conclusion

We demonstrated that puerarin promoted BMSCs proliferation and osteogenic differentiation in vitro and enhanced new bone regeneration in vivo. Our research may serve as an experimental paradigm for the appropriate utilization of puerarin in clinical studies to accelerate bone formation and prevent relapse for RME.

Abbreviations

BMSCs, bone marrow-derived mesenchymal stem cells; RME, rapid maxillary expansion; CCK-8, cell-counting kit-8; ALP, Alkaline phosphatase; BSP, bone sialoprotein; OCN, osteocalcin; Micro-CT, micro-computed tomography; HE, hematoxylin and eosin; BMP2, bone morphogenetic protein 2; MSCs, mesenchymal stem cells; α-MEM, α-minimum essential medium; FBS, fetal bovine serum; PBS, phosphate-buffered saline; BCA, bicinchoninic acid; CPC, cetylpyridinium chloride; RT-PCR, reverse transcriptase polymerase chain reaction; GAPDH, glyceraldehyde-3-phosphate dehydrogenase; Col I, Collagen I; DMSO, dimethyl sulfoxide; AOD, average optical density; DO, distraction osteogenesis; LED, light-emitting diode; RANKL, receptor activator of nuclear factor κ-B ligand; OPG, osteoprotegerin; MCP-1, monocyte chemotactic protein-1; NO, nitric oxide.

Acknowledgments

Disclosure

The authors report no conflicts of interest in this work.

References

1. Gugliandolo A, Fonticoli L, Trubiani O, et al. Oral bone tissue regeneration: mesenchymal stem cells, secretome, and biomaterials. *Int J Mol Sci*. 2021;22(10):5236. doi:10.3390/ijms22105236
2. Brown C, McKee C, Bakshi S, et al. Mesenchymal stem cells: cell therapy and regeneration potential. *J Tissue Eng Regen Med*. 2019;13(9):1738–1755. doi:10.1002/term.2914
3. Tatullo M, Marrelli M, Paduano F. The regenerative medicine in oral and maxillofacial surgery: the most important innovations in the clinical application of mesenchymal stem cells. *Int J Med Sci*. 2015;12(1):72–77. doi:10.7150/ijms.10706
4. Vasanthan J, Gurusamy N, Rajasingh S, et al. Role of human mesenchymal stem cells in regenerative therapy. *Cells*. 2020;10(1):54. doi:10.3390/cells10010054
5. Diomede F, Marconi GD, Cavalcanti MFXB, et al. VEGF/VEGF-R/RUNX2 upregulation in human periodontal ligament stem cells seeded on dual acid etched titanium disk. *Materials*. 2020;13(3):706. doi:10.3390/ma13030706
6. Berebichez-Fridman R, Montero-Olvera PR. Sources and clinical applications of mesenchymal stem cells: state-of-the-art review. *Sultan Qaboos Univ Med J*. 2018;18(3):e264–e277. doi:10.18295/squmj.2018.18.03.002
7. Takigawa M. CCN2: a master regulator of the genesis of bone and cartilage. *J Cell Commun Signal*. 2013;7(3):191–201. doi:10.1007/s12079-013-0204-8
8. Fu J, Wang Y, Jiang Y, et al. Systemic therapy of MSCs in bone regeneration: a systematic review and meta-analysis. *Stem Cell Res Ther*. 2021;12(1):377. doi:10.1186/s13287-021-02456-w
9. Berendsen AD, Olsen BR. Bone development. *Bone*. 2015;80:14–18. doi:10.1016/j.bone.2015.04.035
10. Percival CJ, Richtsmeier JT. Angiogenesis and intramembranous osteogenesis. *Dev Dyn*. 2013;242(8):909–922. doi:10.1002/dvdy.23992
11. Schendel SA, Eisenfeld J, Bell WH, et al. The long face syndrome: vertical maxillary excess. *Am J Orthod*. 1976;70(4):398–408. doi:10.1016/0002-9416(76)90112-3
12. da Silva Filho OG, Boas MC, Capelozza Filho L. Rapid maxillary expansion in the primary and mixed dentitions: a cephalometric evaluation. *Am J Orthod Dentofacial Orthop*. 1991;100(2):171–179. doi:10.1016/S0889-5406(05)81524-0
13. Starnbach H, Bayne D, Cleall J, et al. Facioskeletal and dental changes resulting from rapid maxillary expansion. *Angle Orthod*. 1966;36(2):152–164. doi:10.1043/0003-3219(1966)036<0152:FADCRF>2.0.CO;2

14. Arvystas MG. The rationale for early orthodontic treatment. *Am J Orthod Dentofacial Orthop*. 1998;113(1):15–18. doi:10.1016/S0889-5406(98)70271-9

15. Canan S, Şenışık NE. Comparison of the treatment effects of different rapid maxillary expansion devices on the maxilla and the mandible. Part 1: evaluation of dentoalveolar changes. *Am J Orthod Dentofacial Orthop*. 2017;151(6):1125–1138. doi:10.1016/j.ajodo.2016.11.022

16. Lima AL, Lima Filho RM, Bolognese AM. Long-term clinical outcome of rapid maxillary expansion as the only treatment performed in class I malocclusion. *Angle Orthod*. 2005;75(3):416–420. doi:10.1043/0003-3219(2005)75[416:LCOORM]2.0.CO;2

17. Zimring JF, Isaacson RJ. Forces produced by rapid maxillary expansion. 3. Forces present during retention. *Angle Orthod*. 1965;35:178–186. doi:10.1043/0003-3219(1965)035<0178:FPBRME>2.0.CO;2

18. Hicks EP. Slow maxillary expansion. A clinical study of the skeletal versus dental response to low-magnitude force. *Am J Orthod*. 1978;73(2):121–141. doi:10.1016/0002-9416(78)90183-5

19. Ferreira FN, Gondim JO, Neto JJSM, et al. Effects of low-level laser therapy on bone regeneration of the midpalatal suture after rapid maxillary expansion. *Lasers Med Sci*. 2016;31(5):907–913. doi:10.1007/s10103-016-1933-8

20. Uysal T, Amasyali M, Olmez H, et al. Effect of vitamin C on bone formation in the expanded inter-premaxillary suture. Early bone changes. *J Orofac Orthop*. 2011;72(4):290–300. doi:10.1007/s00056-011-0034-3

21. Li J, Wang X, Wang Y, et al. Isoquercitrin, a flavonoid glucoside, exerts a positive effect on osteogenesis in vitro and in vivo. *Chem Biol Interact*. 2019;297:85–94. doi:10.1016/j.cbi.2018.10.018

22. Birlik M, Babacan H, Cevit R, et al. Effect of sex steroids on bone formation in an orthopedically expanded suture in rats: an immunohistochemical and computed tomography study. *J Orofac Orthop*. 2016;77(2):94–103. doi:10.1007/s00056-016-0021-9

23. Cesur MG, Gülle K, Şirin FB, et al. Effects of curcumin and melatonin on bone formation in orthopedically expanded suture in rats: a biochemical, histological and immunohistochemical study. *Orthod Craniofac Res*. 2018;21:160–167. doi:10.1111/ocr.12232

24. Zhou YX, Zhang H, Peng C. Puerarin: a review of pharmacological effects. *Phytother Res*. 2014;28(7):961–975. doi:10.1002/ptr.5083

25. Zhang Y, Yang X, Ge X, et al. Puerarin attenuates neurological deficits via Bcl-2/Bax/cleaved caspase-3 and Sirt3/SOD2 apoptotic pathways in subarachnoid hemorrhage mice. *Biomed Pharmacother*. 2019;109:726–733. doi:10.1016/j.biopha.2018.10.161

26. Sun XH, Ding J-P, Li H, et al. Activation of large-conductance calcium-activated potassium channels by puerarin: the underlying mechanism of puerarin-mediated vasodilation. *J Pharmacol Exp Ther*. 2007;323(1):391–397. doi:10.1124/jpet.107.125567

27. Zhang Q, Huang W, Lv X, et al. Puerarin protects differentiated PC12 cells from H$_2$O$_2$-induced apoptosis through the PI3K/Akt signalling pathway. *Cell Biol Int*. 2012;36(5):419–426. doi:10.1042/CBI20100900

28. Lee OH, Seo D-H, Park C-S, et al. Puerarin enhances adipocyte differentiation, adiponectin expression, and antioxidant response in 3T3-L1 cells. *Biofactors*. 2010;36(6):459–467. doi:10.1002/biof.119

29. Bo J, Ming BY, Gang LZ, et al. Protection by puerarin against MPP+-induced neurotoxicity in PC12 cells mediated by inhibiting mitochondrial dysfunction and caspase-3-like activation. *Neurosci Res*. 2005;53(2):183–188. doi:10.1016/j.neures.2005.06.014

30. Zou Y, Hong B, Fan L, et al. Protective effect of puerarin against beta-amyloid-induced oxidative stress in neuronal cultures from rat hippocampus: involvement of the GSK-3β/Nrf2 signaling pathway. *Free Radic Res*. 2013;47(1):55–63. doi:10.3109/10715762.2012.742518

31. Xiao L, Zhong M, Huang Y, et al. Puerarin alleviates osteoporosis in the ovariectomy-induced mice by suppressing osteoclastogenesis via inhibition of TRAF6/ROS-dependent MAPK/NF-κB signaling pathways. *Aging*. 2020;12(21):21706–21729. doi:10.18632/aging.103976

32. Yang S, Lou JL, Wang Q. [Effect of puerarin on liver injury in KKAy mice with type 2 diabetes mellitus]. *Zhongguo Zhong Xi Yi Jie He Za Zhi*. 2009;29(8):707–710. Chinese.

33. Zhou Y, Lian H, Liu K, et al. Puerarin improves graft bone defect through microRNA-155-3p-mediated p53/TNF-α/STAT1 signaling pathway. *Int J Mol Med*. 2020;46(1):239–251. doi:10.3892/ijmm.2020.4595

34. Wong R, Rabie B. Effect of puerarin on bone formation. *Osteoarthritis Cartilage*. 2007;15(8):894–899. doi:10.1016/j.joca.2007.02.009

35. Ilizarov GA, Soĭbel'man LM. [Clinical and experimental data on bloodless lengthening of lower extremities]. *Eksp Khir Anesteziol*. 1969;14(4):27–32. Russian.

36. Sailhan F. Bone lengthening (distraction osteogenesis): a literature review. *Osteoporos Int*. 2011;22(6):2011–2015. doi:10.1007/s00198-011-1613-2

37. Rosa CB, Habib FAL, de Araújo TM, et al. Laser and LED phototherapy on midpalatal suture after rapid maxilla expansion: Raman and histological analysis. *Lasers Med Sci*. 2017;32(2):263–274. doi:10.1007/s10103-016-2108-3

38. Zhao S, Wang X, Li N, et al. Effects of strontium ranelate on bone formation in the mid-palatal suture after rapid maxillary expansion. *Drug Des Devel Ther*. 2015;9:2725–2734. doi:10.2147/DDDT.S82892

39. Li H, Chen B, Pang G, et al. Anti-osteoporotic activity of puerarin 6″-O-xyloside on ovariectomized mice and its potential mechanism. *Pharm Biol*. 2016;54(1):111–117. doi:10.3109/13880209.2015.1017885

40. Sheu SY, Tsai -C-C, Sun J-S, et al. Stimulatory effect of puerarin on bone formation through co-activation of nitric oxide and bone morphogenetic protein-2/mitogen-activated protein kinases pathways in mice. *Chin Med J*. 2012;125(20):3646–3653.

41. Yang X, Yang Y, Zhou S, et al. Puerarin stimulates osteogenic differentiation and bone formation through the ERK1/2 and p38-MAPK signaling pathways. *Curr Mol Med*. 2018;17(7):488–496. doi:10.2174/1566524018666171219101142

42. Wang PP, Zhu X-F, Yang L, et al. Puerarin stimulates osteoblasts differentiation and bone formation through estrogen receptor, p38 MAPK, and Wnt/β-catenin pathways. *J Asian Nat Prod Res*. 2012;14(9):897–905. doi:10.1080/10286020.2012.702757

43. Zhang Y, Zeng X, Zhang L, et al. Stimulatory effect of puerarin on bone formation through activation of PI3K/Akt pathway in rat calvaria osteoblasts. *Planta Med*. 2007;73(4):341–347. doi:10.1055/s-2007-967168

44. Zhang Y, Yan M, Yu Q-F, et al. Puerarin prevents LPS-induced osteoclast formation and bone loss via inhibition of Akt activation. *Biol Pharm Bull*. 2016;39(12):2028–2035. doi:10.1248/bpb.b16-00522

45. Lin S, Ke D, Lin Y, et al. Puerarin inhibits the migration of osteoclast precursors and osteoclastogenesis by inhibiting MCP-1 production. *Biosci Biotechnol Biochem*. 2020;84(7):1455–1459. doi:10.1080/09168451.2020.1738912

46. Tiyasatkulkovit W, Malaivijitnond S, Charoenphandhu N, et al. Pueraria mirifica extract and puerarin enhance proliferation and expression of alkaline phosphatase and type I collagen in primary baboon osteoblasts. *Phytomedicine*. 2014;21(12):1498–1503. doi:10.1016/j.phymed.2014.06.019

47. Seibel MJ. Biochemical markers of bone turnover: part I: biochemistry and variability. *Clin Biochem Rev*. 2005;26(4):97–122.

48. Moser SC, van der Eerden BCJ. Osteocalcin-A versatile bone-derived hormone. *Front Endocrinol*. 2018;9:794. doi:10.3389/fendo.2018.00794

49. Nakashima K, Zhou X, Kunkel G, et al. The novel zinc finger-containing transcription factor osterix is required for osteoblast differentiation and bone formation. *Cell*. 2002;108(1):17–29. doi:10.1016/S0092-8674(01)00622-5

50. Wang Y, Zhang X, Shao J, et al. Adiponectin regulates BMSC osteogenic differentiation and osteogenesis through the Wnt/β-catenin pathway. *Sci Rep*. 2017;7(1):3652. doi:10.1038/s41598-017-03899-z

51. Shen G, Ren H, Shang Q, et al. Foxf1 knockdown promotes BMSC osteogenesis in part by activating the Wnt/β-catenin signalling pathway and prevents ovariectomy-induced bone loss. *EBioMedicine*. 2020;52:102626. doi:10.1016/j.ebiom.2020.102626

52. Duan P, Bonewald LF. The role of the wnt/β-catenin signaling pathway in formation and maintenance of bone and teeth. *Int J Biochem Cell Biol*. 2016;77(Pt A):23–29. doi:10.1016/j.biocel.2016.05.015

53. Sen B, Paradise CR, Xie Z, et al. β-Catenin preserves the stem state of murine bone marrow stromal cells through activation of EZH2. *J Bone Miner Res*. 2020;35(6):1149–1162. doi:10.1002/jbmr.3975

54. Linsley C, Wu B, Tawil B. The effect of fibrinogen, collagen type I, and fibronectin on mesenchymal stem cell growth and differentiation into osteoblasts. *Tissue Eng Part A*. 2013;19(11–12):1416–1423. doi:10.1089/ten.tea.2012.0523

55. Akhir HM, Teoh PL. Collagen type I promotes osteogenic differentiation of amniotic membrane-derived mesenchymal stromal cells in basal and induction media. *Biosci Rep*. 2020;40(12). doi:10.1042/BSR20201325

56. Arai Y, Choi B, Kim BJ, et al. Cryptic ligand on collagen matrix unveiled by MMP13 accelerates bone tissue regeneration via MMP13/Integrin α3/RUNX2 feedback loop. *Acta Biomater*. 2021;125:219–230. doi:10.1016/j.actbio.2021.02.042

57. Ziros PG, Basdra EK, Papavassiliou AG. Runx2: of bone and stretch. *Int J Biochem Cell Biol*. 2008;40(9):1659–1663. doi:10.1016/j.biocel.2007.05.024

58. Chuang LS, Ito K, Ito Y. RUNX family: regulation and diversification of roles through interacting proteins. *Int J Cancer*. 2013;132(6):1260–1271. doi:10.1002/ijc.27964

59. Almalki SG, Agrawal DK. Key transcription factors in the differentiation of mesenchymal stem cells. *Differentiation*. 2016;92(1–2):41–51. doi:10.1016/j.diff.2016.02.005

60. Chatterjee M, Faot F, Correa C, et al. A robust methodology for the quantitative assessment of the rat jawbone microstructure. *Int J Oral Sci*. 2017;9(2):87–94. doi:10.1038/ijos.2017.11

61. Sato M, Yasui N, Nakase T, et al. Expression of bone matrix proteins mRNA during distraction osteogenesis. *J Bone Miner Res*. 1998;13 (8):1221–1231. doi:10.1359/jbmr.1998.13.8.1221

62. Aronson J. Experimental and clinical experience with distraction osteogenesis. *Cleft Palate Craniofac J*. 1994;31(6):473–481. doi:10.1597/1545-1569_1994_031_0473_eacewd_2.3.co_2

63. Kloen P, Lauzier D, Hamdy RC. Co-expression of BMPs and BMP-inhibitors in human fractures and non-unions. *Bone*. 2012;51(1):59–68. doi:10.1016/j.bone.2012.03.032

64. Zhang J, Lazarenko OP, Wu X, et al. Differential effects of short term feeding of a soy protein isolate diet and estrogen treatment on bone in the pre-pubertal rat. *PLoS One*. 2012;7(4):e35736. doi:10.1371/journal.pone.0035736

65. Harris H. The human alkaline phosphatases: what we know and what we don't know. *Clin Chim Acta*. 1990;186(2):133–150. doi:10.1016/0009-8981(90)90031-M

66. Hu X, Sun Z, Li F, et al. Burn-induced heterotopic ossification from incidence to therapy: key signaling pathways underlying ectopic bone formation. *Cell Mol Biol Lett*. 2021;26(1):34. doi:10.1186/s11658-021-00277-6

67. Dey D, Wheatley BM, Cholok D, et al. The traumatic bone: trauma-induced heterotopic ossification. *Transl Res*. 2017;186:95–111. doi:10.1016/j.trsl.2017.06.004

68. Evans KN, Potter BK, Brown TS, et al. Osteogenic gene expression correlates with development of heterotopic ossification in war wounds. *Clin Orthop Relat Res*. 2014;472(2):396–404. doi:10.1007/s11999-013-3325-8